KØRSCH OPTICS, INC.
10111 BLUFF DRIVE, HUNTSVILLE, ALABAMA 35803
(205) 881-1166

(NASA-CR-170950) TECHNICAL SUPPORT FOR AXAF Final Report (Korsch Optics, Inc.) 24 p HC A02/MF A01 CSCL 20F
N84-15959
Unclas
G3/74 43330

TECHNICAL SUPPORT FOR AXAF

FINAL REPORT

PREPARED FOR

NATIONAL AERONAUTICS AND SPACE ADMINISTRATION

MARSHALL SPACE FLIGHT CENTER, ALABAMA

CONTRACT NAS8-34943

NOVEMBER 1983

TECHNICAL SUPPORT FOR AXAF

This report summarizes the results of a study effort performed under contract No.: NAS8-34943. The report is divided into two parts. The first part describes the effcts of ray aberrations due to various surface errors on the point image , and the second part introduces a new method and rationale for optimizing the performance of nested arrays of grazing incidence telescopes.

I. RAY ABERRATIONS DUE TO SURFACE ERRORS

As part of the overall error analysis of the AXAF telescope assembly this is an attempt to describe and categorize the low frequency, aberration causing surface defects in the most general manner.

This work compliments the analysis done by SAO/High Energy Astrophysics Division which is based on assuming selected geometric deformations.

A half meridional section of a two-mirror grazing incidence configuration including the basic design parameters is shown in fig.1.

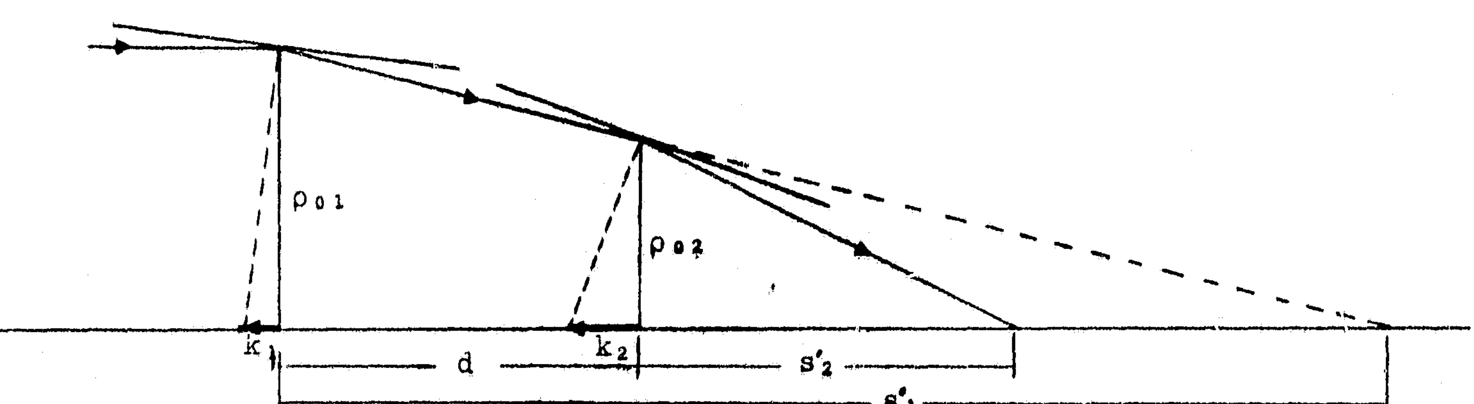

Fig.1: Two-mirror grazing incidence configuration

A meridional section of a real, slightly deformed surface may be represented by the equation

$$\rho = \sqrt{\rho_0^2 + 2kz - \psi z^2} + e_0 + e_1 z + e_2 z^2 + \ldots + e_i z^i + \ldots \qquad (1)$$

where the square root term represents the ideal design surface and the remaining terms make up the surface error function. Since the distributions of surface defects will generally not be rotationally symmetric, they are also a function of the azimuth angle, ϕ, i.e.,

$$e_i = e_{i0} + e_{i1}\phi + e_{i2}\phi^2 + \ldots + e_{ij}\phi^j + \ldots \qquad (2)$$

so that the complete set of error terms can be summarized as follows:

$$\Delta\rho(z,\phi) = \sum_{i=0}^{\infty}\left(\sum_{j=0}^{\infty} e_{ij}\phi^j\right) z^i \qquad (3)$$

We now divide the total into three main categories of surface errors:

1. Radial Error: $\Delta\rho = \Delta\rho(z,\phi)$

2. Axial Slope Error: $\Delta\alpha = \dfrac{\Delta\rho(z,\phi)}{z}$

3. Circumferential Slope Error: $\Delta\phi = \dfrac{\Delta\rho(z,\phi)}{\rho\ \phi}$

I Radial Surface Error

The radial error can be divided into two components:

a) a constant component: $\Delta\rho=\Delta\rho_0=e_{00}$

b) a variable component: $\Delta\rho=\Delta\rho(z,\phi)-e_{00}$

To determine the ray aberration caused by a local error in radius, $\Delta\rho$, we refer to fig.2.

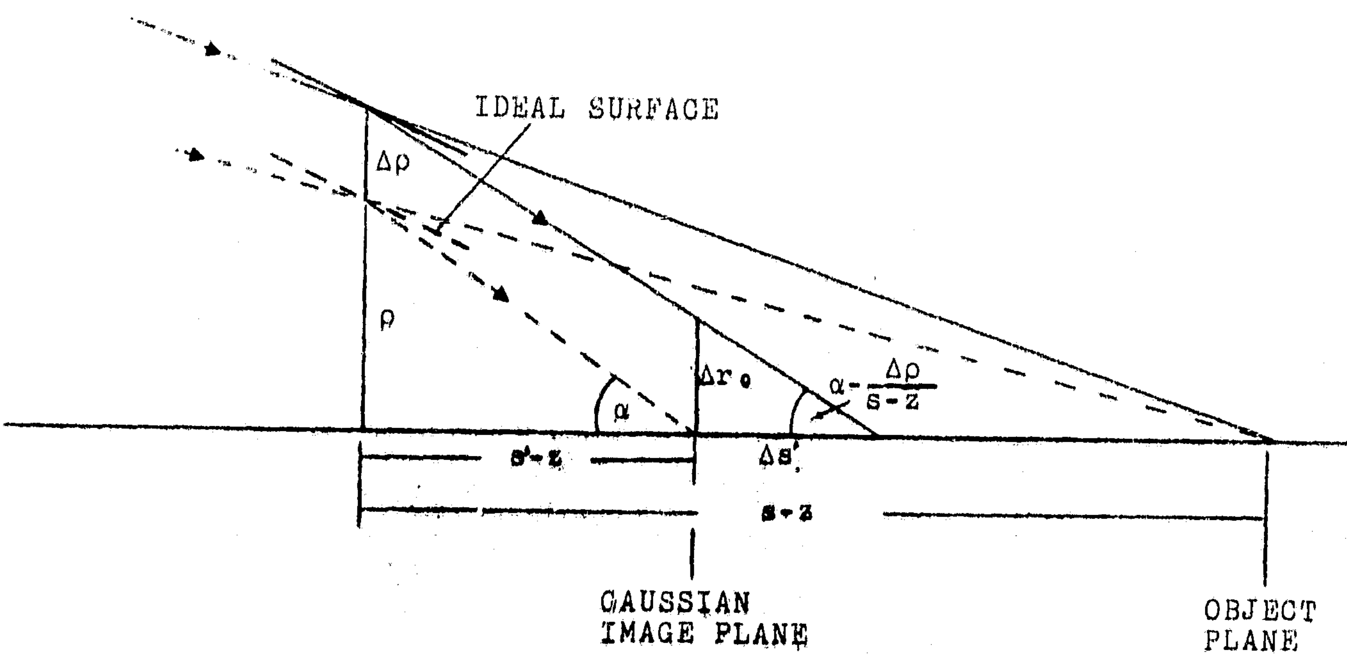

Fig.2: Ray aberration due to radial surface error

Since α is a small angle we have

$$\alpha = \frac{\rho}{s'-z} \tag{4}$$

and

$$\alpha - \frac{\Delta\rho}{s-z} = \frac{\rho+\Delta\rho}{s'-z+\Delta s'} \tag{5}$$

Eliminating α by combining eqs. 4 and 5 yield

$$\Delta s' = \frac{\Delta\rho}{\rho}\left(1+\frac{s'-z}{s-z}\right)(s'-z) \qquad (6)$$

Using the surface equation,

$$\rho^2 \approx \rho_0^2 + 2kz \qquad (7)$$

and the lens equation

$$\frac{2k}{\rho_0^2} \approx -\frac{1+m}{2s'}\quad , \quad \left(m=\frac{s'}{s}\right) \qquad (8)$$

one obtains
$$\rho^2 = \rho_0^2\left[1-(1+m)\frac{z}{s'}\right] \qquad (9)$$

or
$$\rho \approx \rho_0\left[1-\frac{1+m}{2}\,\frac{z}{s'}\right] \qquad (10)$$

Eq. 10 inserted into eq.6 gives

$$\Delta s' \approx \frac{s'\Delta\rho}{\rho_0}\left(1+\frac{s'-z}{s-z}\right)\left(1+\frac{1+m}{2}\,\frac{z}{s'}\right)\left(1-\frac{z}{s'}\right) \qquad (11)$$

which yields after developing and neglecting all non-linear terms of $\frac{z}{s'}$,

$$\Delta s' \approx \frac{s'}{\rho_0}\left[(1+m)-(1-m)(3m+1)\frac{z}{2s'}\right]\Delta\rho \qquad (12)$$

Eq. 12 applied to primary and secondary gives to the first order $(\frac{z}{s'} \approx o)$:

1. Primary $(m_1=0)$

longitudinal aberration: $\Delta s_1' = \frac{s_1'}{\rho_{01}}\,\Delta\rho$ (13)

lateral aberration : $\Delta r_{01} = \Delta\rho$ (14)

In the final focal plane the lateral aberration becaomes

$$\Delta r_0 = m_2 \Delta r_{01} = \frac{\Delta\rho}{2} \tag{15}$$

or, in angular units

$$\Delta\gamma_0 = \frac{\Delta\rho}{2f} \; [\mathrm{rad}] \tag{16}$$

2. Secondary ($m_2 = \frac{1}{2}$)

longitudinal aberration: $\Delta s_2' = \frac{3}{2} \frac{s_2'}{\rho_{02}} \Delta\rho$ (17)

lateral aberration : $\Delta r_{02} = \frac{3}{2} \Delta\rho$ (18)

or, in angular units $\Delta\gamma_0 = \frac{3\Delta\rho}{2f} \; [\mathrm{rad}]$ (19)

A special situation exists when $\Delta\rho = \Delta\rho_0$ is constant over the entire surface. This results primarily in a focal shift and in a small amount of spherical aberration.

The longitudinal aberration is formed by the two marginal rays reflected at $z=-z_0$ and $z=+z_0$. Using eq. 12 we obtain

$$\Delta\Delta s' = \Delta s'(-z_0) - \Delta s'(+z_0) = \frac{z_0}{\rho_0}(1-m)(3m+1)\Delta\rho_0 \tag{20}$$

(see fig.3)

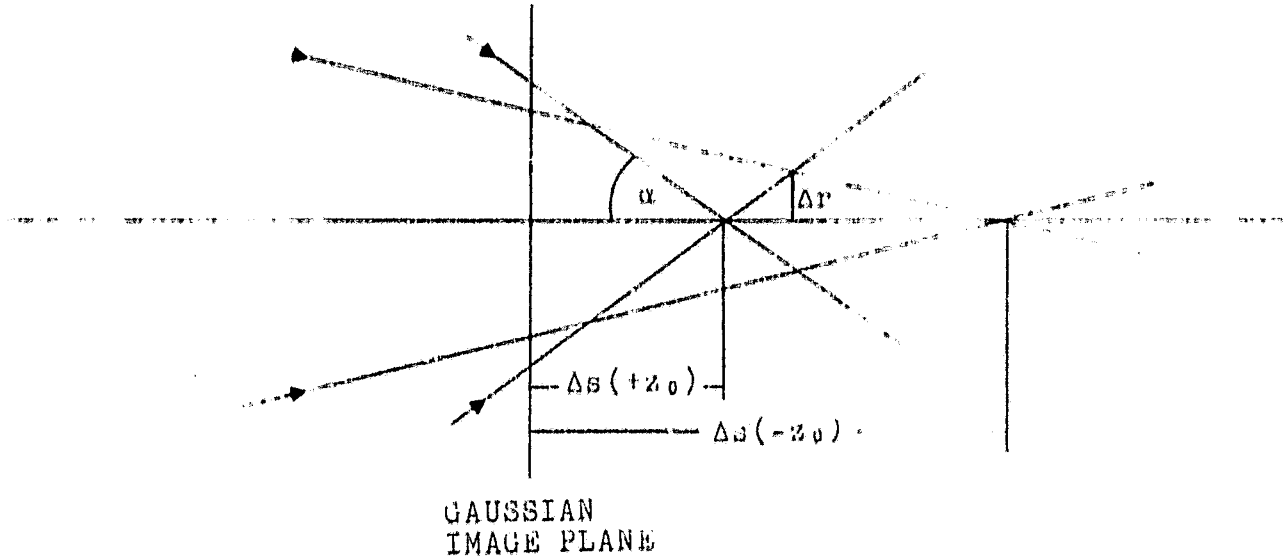

Fig.3: Focal shift and circle of least confusion due to a constant radial error

Applied to the two surfaces we obtain:

1. Primary ($m_1=0$)

Mean focal shift (for $z_1=0$, $\rho_1=\rho_{01}$): $\overline{\Delta s}'_1 = \frac{s'_1}{\rho_{01}} \Delta\rho_0$ (21)

longitudinal aberration : $\Delta\Delta s'_1 = \frac{z_{01}}{\rho_{01}} \Delta\rho_0$ (22)

radius of circle of least confusion: $\Delta r_1 \approx \alpha \frac{\Delta\Delta s'_1}{2} \approx \frac{\rho_{01}}{2s'_1} \cdot \frac{z_{01}}{\rho_{01}} \Delta\rho_0$

$$= \frac{z_{01}}{2s'_1} \Delta\rho_0 \qquad (23)$$

For best performance the first focus of the secondary must coincide with the location of the circle of least confusion. This is achieved by adjusting the mirror separation, d, by the amount

$$\Delta d = \overline{\Delta s_1'} = \frac{s_1'}{\rho_{01}} \Delta\rho_0 \tag{24}$$

Then the diameter of the circle of least confusion in the final focal plane is

$$2\Delta r = m_2 \frac{z_{01}}{s_1'} \Delta\rho_0 = \frac{z_{01}}{2s_1'} \Delta\rho_0 \tag{25}$$

In angular units it is

$$2\Delta\gamma = \frac{z_{01}}{2s_1} \frac{\Delta\rho_0}{f} \left[\text{rad}\right] \tag{26}$$

or, since $s_1' = f/m_2$ and $m_2 = \frac{1}{2}$,

$$2\Delta\gamma = \frac{z_{01}}{(2f)^2} \Delta\rho_0 \left[\text{rad}\right] \tag{27}$$

2. Secondary ($m_2 = \frac{1}{2}$)

Mean focal shift($z_2=0$, $\rho_2=\rho_{02}$): $\overline{\Delta s_2'} = \frac{3}{2} \frac{s_2'}{\rho_{02}} \Delta\rho_0$ (28)

longitudinal aberration : $\Delta\Delta s_2' = \frac{5}{4} \frac{z_{02}}{\rho_{02}} \Delta\rho_0$ (29)

radius of circle of least confusion: $\Delta r_2 = \frac{5}{8} \frac{z_{02}}{s_1'} \Delta\rho_0$ (30)

The diameter of the circle of least confusion is then

$$2\Delta r = \frac{5}{4} \frac{z_{02}}{s_2'} \Delta\rho_0 \tag{31}$$

or in angular units

$$2\Delta\gamma = \frac{5}{4} \frac{z_{02}}{s_2' f} \Delta\rho_0 \left[\text{rad}\right] \tag{32}$$

ORIGINAL PAGE IS
OF POOR QUALITY

II Axial Slope Error

The axial slope error can also be divided into two components:

a) a constant component: $\Delta\alpha=\Delta\alpha_0=e_{20}$

b) a variable component: $\Delta\alpha=\frac{\partial\Delta\rho}{\partial z}-e_{10}$

To determine the longitudinal and lateral ray aberration caused by a local axial slope error we refer to fig.4.

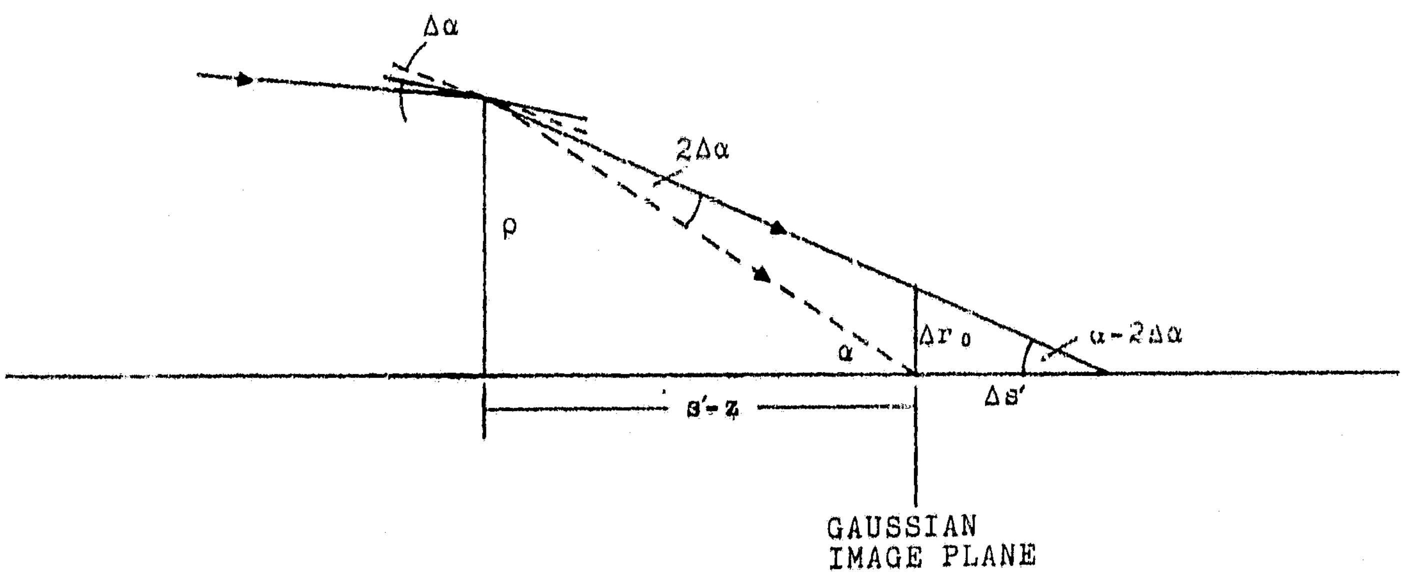

Fig.4: Ray aberration due to an axial slope error

It is

$$\alpha-2\Delta\alpha=\frac{\rho}{s'-z+\Delta s'} \tag{32}$$

or

$$\Delta s'=\frac{\rho}{\alpha-2\Delta\alpha}-(s'-z)\approx\frac{\rho}{\alpha}(1+2\frac{\Delta\alpha}{\alpha})-(s'-z) \tag{33}$$

It is also

$$\alpha=\frac{\rho}{s'-z} \tag{34}$$

Eq.34 inserted into eq. 33 gives

$$\Delta s' = \frac{2\Delta\alpha}{\rho}\,(s'-z)^2 \tag{35}$$

Finally, after replacing ρ by eq.10 one obtains

$$\Delta s' = \frac{2s'^2}{\rho_0}\left[1+\frac{z}{2s'}(m-3)\right]\Delta\alpha \tag{36}$$

Eq. 32 applied to primary and secondary gives to the first order:

1. Primary($m_1=0$)

   longitudinal aberration: $\Delta s_1' = 2\frac{s_1'^2}{\rho_{01}}\,\Delta\alpha$ (37)

   lateral aberration : $\Delta r_{01} = 2s_1'\Delta\alpha$ (38)

In the final focal plane the lateral ray aberration becomes

$$\Delta r_0 = m_2\Delta r_{01} = s_1'\Delta\alpha \tag{39}$$

In angular units

$$\Delta\gamma_0 = \frac{s_1'}{f}\,\Delta\alpha\,[\mathrm{rad}] \tag{40}$$

or, since $s_1' = f/m_2 = 2f$

$$\Delta\gamma_0 = 2\Delta\alpha\,[\mathrm{rad}] \tag{41}$$

2. Secondary ($m_2=\frac{1}{2}$)

   longitudinal aberration: $\Delta s_2' = 2\frac{s_2'^2}{\rho_{02}}\,\Delta\alpha$ (42)

   lateral aberration : $\Delta r_{02} = 2s_2'\,\Delta\alpha$ (43)

   or, in angular units : $\Delta\gamma_0 = 2\frac{s_2'}{f}\,\Delta\alpha$ (44)

   $= 2\frac{\rho_{02}}{\rho_{01}}\,\Delta\alpha$

A special situation exists again when $\Delta\alpha$ $\Delta\alpha_0$ is constant over the entire surface. This results also primarily in a focus shift and in a small amount of spherical aberration.

The error function causing a constant axial slope error is $\Delta\rho=\Delta\alpha_0 z$, i.e., there is a radial error of the amount $\Delta\alpha_0 z$ associated with the slope error which results according to eq. 1 in an additional focal shift of $\frac{s'}{\rho_0}(1+m)z\Delta\alpha_0$. This amount must be added to eq. 36 for the total focal shift.

$$\Delta s'=\frac{2s'^2}{\rho_0}\left[1+(m-3)\frac{z}{2s'}\right]\Delta\alpha_0+\frac{s'}{\rho_0}(1+m)\frac{z}{s'}\Delta\alpha_0$$

$$=\frac{2s'^2}{\rho_0}\left[1+(m-1)\frac{z}{s'}\right]\Delta\alpha_0 \qquad (45)$$

The longitudinal aberration is formed by the two marginal rays reflected at $z=-z_0$ off the surface. Using eq. 45 one obtains for the longitudinal aberration, (see fig.5)

$$\Delta\Delta s'=\Delta s'(-z_0)-\Delta s'(+z_0)=\frac{2s'z_0}{\rho}(1-m)\Delta\alpha_0 \qquad (46)$$

Applied to the two surfaces we obtain:

1. Primary ($m_1=0$)

   Mean focal shift($z_1=0, \rho_1=\rho_{01}$): $\overline{\Delta s}_1'=2\frac{s_1'^2}{\rho_{01}}\Delta\alpha_0$ (47)

   longitudinal aberration : $\Delta\Delta s_1'=4\frac{s_1' z_{01}}{\rho_{01}}\Delta\alpha_0$ (48)

   radius of circle of least confusion : $\Delta r_1=\frac{\Delta\Delta s_1'}{2}\alpha=2z_{01}\Delta\alpha_0$ (49)

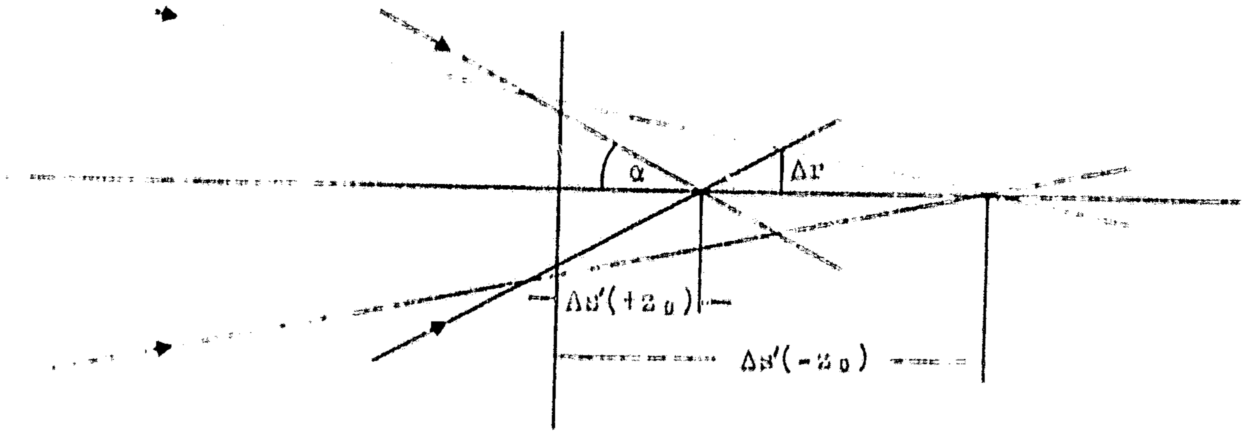

GAUSSIAN
IMAGE PLANE

Fig.5: Focal shift and circle of least confusion due to a constant axial slope error

To match the first focus of the secondary with the location of the circle of least confusion the mirror separation, d, must be adjusted by the amount

$$\Delta d=\overline{\Delta s}'_1=\overset{2}{\cancel{4}}\frac{a_1^2}{\rho_{01}}\Delta\alpha_0 \tag{50}$$

Thus the diameter of the circle of least confusion in the final focal plane is

$$2\Delta r=4m_2 z_{01}\Delta\alpha_0=2z_{01}\Delta\alpha_0 \tag{51}$$

or in angular units,

$$2\Delta\gamma=\frac{2z_0}{f}\Delta\alpha_0 \;\left[\text{rad}\right] \tag{52}$$

2. Secondary $(m_2=\frac{1}{2})$

Mean focal shift $(z_1=0, \rho_1=\rho_{01})$: $\overline{\Delta s}'_2=-2\frac{s_2'^2}{\rho_{02}}\Delta\alpha_0$ (53)

longitudinal aberration : $\Delta\Delta s'_2=2\frac{s'_2 z_{02}}{\rho_{02}}\Delta\alpha_0$ (54)

radius of circle of least confusion : $\Delta r_2=\frac{\Delta\Delta s'_2}{2}\alpha=z_{02}\Delta\alpha_0$ (55)

The diameter of the circle of least confusion is then

$$2\Delta r=2z_{02}\Delta\alpha_0 \tag{56}$$

or in angular units

$$2\Delta\gamma=2\frac{z_{02}}{f}\Delta\alpha_0 \tag{57}$$

It may be mentioned here that ray trace results showed that the spherical aberration due to a constant axial slope error can be completely compensated by an appropriate separation change, Δd. For the primary this is

$$\Delta d=\frac{1}{2}\overline{\Delta s}'_1=2\frac{s_1'^2}{\rho_{01}}\Delta\alpha_0 \tag{58}$$

and for the secondary $\Delta d=\frac{1}{2m^2}\overline{\Delta s}'_2=-4\frac{s_2'^2}{\rho_{02}}\Delta\alpha_0$ (59)

A similar compensation cannot be made for a constant radial surface error.

III Circumferential Slope Error

A small local circumferential slope error may be represented by a corresponding decenter. Slope error, $\Delta\phi$, and decenter,

Δx, are, in accordance with fig.6 related by

$$\Delta x=\rho\Delta\phi \tag{60}$$

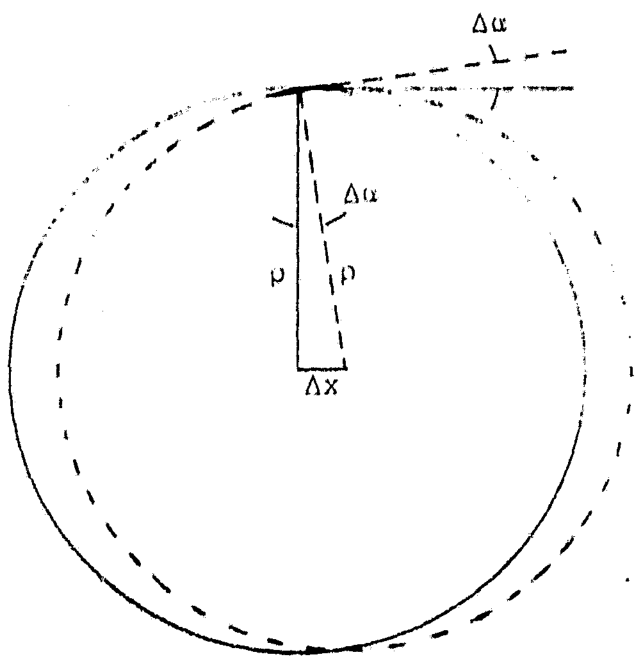

Fig.6: Circumferential Slope error

Applied to primary and secondary we have:

1. Primary

The ray aberration in the primary focal plane is

$$\Delta r_1=\Delta x=\rho_1\Delta\phi \tag{61}$$

and in the final focal plane

$$\Delta r=m_2\Delta r_1=\frac{\rho_1}{2}\Delta\phi \tag{62}$$

or in angular units

$$\Delta\gamma=\frac{\rho_1}{2f}\Delta\phi \quad \left[\mathrm{rad}\right] \tag{63}$$

2. Secondary

The ray aberration in the secondary and final focal plane is

$$\Delta r_2=(m+1)\rho_2\Delta\phi=\frac{3}{2}\rho_2\Delta\phi \tag{64}$$

or in angular units

$$\Delta\gamma=\frac{3\rho_2}{2f}\Delta\phi \tag{65}$$

A constant circumferential slope error amounts to a constant radial change which has been treated in section I.

This work will be continued by applying the results to the AXAF telescope assembly.

ORIGINAL PAGE IS
OF POOR QUALITY

SUMMARY OF RAY ABERRATIONS DUE TO SURFACE ERRORS

This is a summary of the calculated effects of various surface errors on the point image of grazing incidence telescopes applied to the six subsystems of the AXAF Telescope Assembly. In order to write the equations as functionsof the following system parameters,

f: system focal length (f=400in.)
b: back focal distance (b=380in.)
ρ_{01}:center radius of first surface (ρ_{01}=23.88,21.63,19.23 16.98,14.78,12.63 in.)
z_{01}:half length of first surface (z_{01}=15.8 in.)

we make use of the following relations:

$$s_1'=f/2, \quad \frac{\rho_{02}}{\rho_{01}}=\frac{b}{f} \quad \text{and} \quad z_{02}=\frac{b}{f}z_{01}\ .$$

1. Local Radial Surface Error

A local error in the mirror radius, $\Delta\rho$, causes the following ray aberrations in the final Gaussian focal plane:

on the primary: $\Delta\gamma_0=\frac{\Delta\rho}{2f}=0.00125\Delta\rho$ rad

on the secondary: $\Delta\gamma_0=\frac{3\Delta\rho}{2f}=0.00375\Delta\rho$ rad

2. Constant Radial Surface Error

A constant radial surface error, $\Delta\rho_0$, over the entire surface causes a focal shift as well as a small amount of spherical aberration.

On the primary:

diameter of circle of least confusion: $2\Delta\gamma=\frac{z_{01}}{(2f)^2}\Delta\rho_0=2.5\cdot 10^{-5}\Delta\rho_0$ rad

separation change to compensate focal shift: $\Delta d=\frac{2f}{\rho_{01}}\Delta\rho_0=\frac{800}{\rho_{01}}\Delta\rho_0$

on the secondary:

diameter of circle of least confusion: $2\Delta\gamma = \frac{5z_{01}}{(2f)^2}\Delta\rho_0 = 1.25\cdot10^{-4}\Delta\rho_0$ rad

separation change to compensate focal shift: $\Delta d = \frac{6f}{\rho_{01}}\Delta\rho_0 = \frac{2400}{\rho_{01}}\Delta\rho_0$

3. Local Slope Error

A local axial slope error, $\Delta\alpha$, causes the following angular ray aberrations in the final Gaussian focal plane:

on the primary: $\Delta\gamma_0 = 2\Delta\alpha$ rad

on the secondary: $\Delta\gamma_0 = 2\frac{b}{f}\Delta\alpha = 1.9\Delta\alpha$ rad

4. Constant Axial Slope Error

A constant axial slope error, $\Delta\alpha_0$, over the entire surface causes a focal shift and spherical aberration. The spherical aberration can be completely compensated by an appropriate separation change. This results, however, in a final focal plane shift, Δb.

On the primary:

compensating mirror separation: $\Delta d = 4\frac{f^2}{\rho_{01}}\Delta\alpha_0 = 6.4\cdot10^5\frac{\Delta\alpha_0}{\rho_{01}}$

resulting focal shift : $\Delta b = -\frac{f^2}{\rho_{01}}\Delta\alpha_0 = 1.6\cdot10^5\frac{\Delta\alpha_0}{\rho_{01}}$

On the secondary:

compensating mirror separation: $\Delta d = -4\frac{bf}{\rho_{01}}\Delta\alpha_0 = 6.1\cdot10^5\frac{\Delta\alpha_0}{\rho_{01}}$

resulting focal shift : $\Delta b = \frac{bf}{\rho_{01}}\Delta\alpha_0 = 1.5\cdot10^5\frac{\Delta\alpha_0}{\rho_{01}}$

5. Circumferential Slope Error

A local circumferential slope error, $\Delta\phi$, causes the following angular ray aberrations in the final Gaussian focal plane:

on the primary: $\Delta\gamma_0 = \frac{\rho_{01}}{2f}\,\Delta\phi = 0.00125\,\rho_{01}\Delta\phi$ rad

on the secondary: $\Delta\gamma_0 = \frac{3b\rho_{01}}{2f^2} = 0.00356\,\rho_{01}\Delta\phi$ rad

A constant circumferential slope error is equivalent to a constant radial surface error.

ORIGINAL PAGE IS
OF POOR QUALITY

II. OPTIMIZING THE GRAZING INCIDENCE TELESCOPE

Since any attempt to improve the performance of the conventional Wolter-type telescope turns out to be futile, it may be interesting to see what an "ideal" grazing incidence telescope would look like.

The condition for such a system is found by examining its aberrations. The primary aberration of a grazing incidence two-mirror telescope is given by a single term,

$$\Delta\xi' = -\frac{f}{\rho_{01}}(d-2z_1)\phi^2\cos\omega$$

where $\Delta\xi'$ is the lateral ray aberration, f the system focal length, ϕ the half field angle and ω the polar angle in the entrance plane. The remaining quantities are given in fig.1.

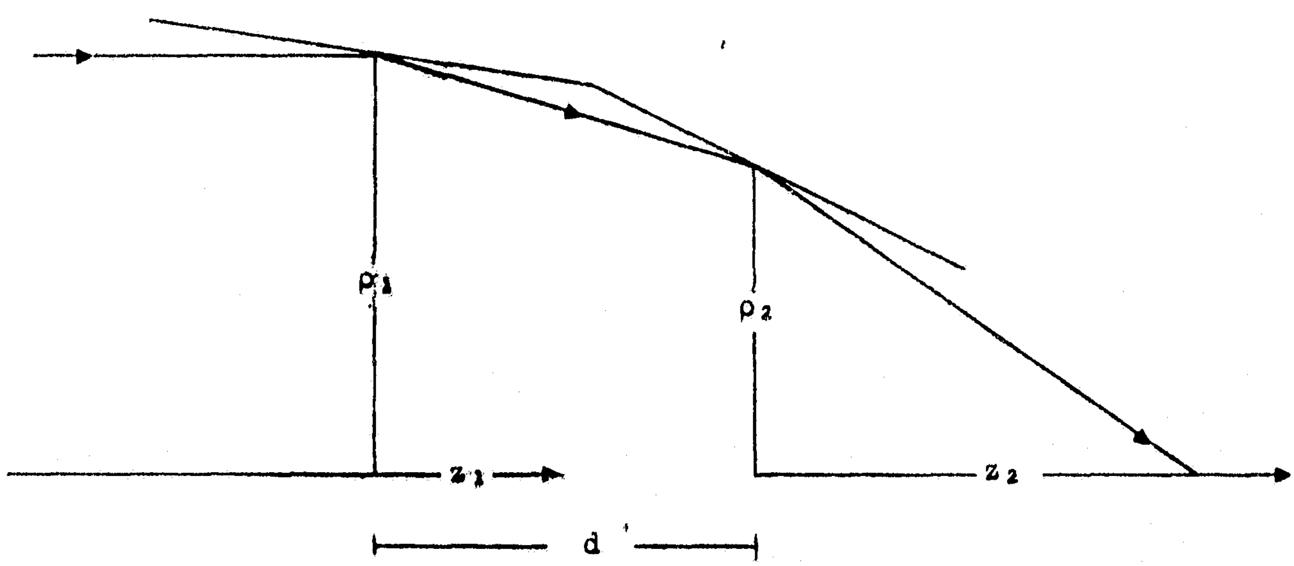

Fig.1: Two-mirror grazing incidence geometry

The aberration term controls the lateral aberration as well as the field curvature; i.e., both decrease linearly toward the intersection of primary and secondary, and disappear for $z_1 = {}^d/_2$. Optimum performance is, therefore, obtained in the vicinity where the two surfaces adjoin. The concept of such a short element system is shown in fig. 2. Obviously, the shorter the element length, the less the collecting area per element, and a large number of rings are required for a sufficiently large total collecting area.

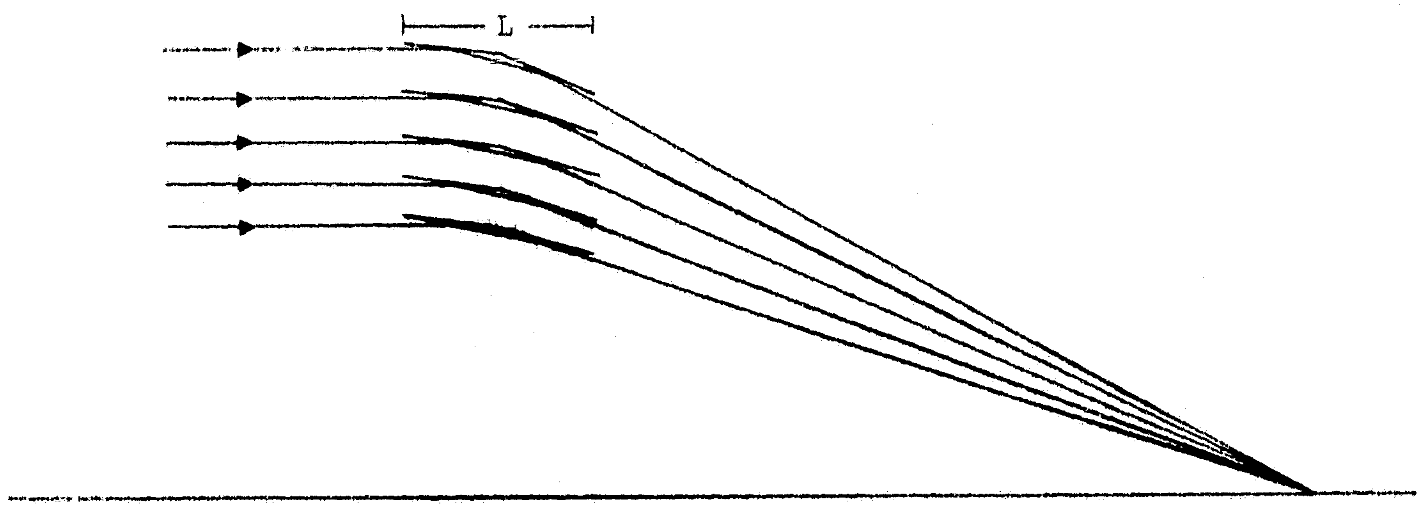

Fig.2: Conceptual drawing of a short element grazing incidence telescope.

As an example a system was analyzed consisting of 100 4 in. long elements with radii between 14 in. and 24 in. yielding about the same accumulative collecting area as AXAF.

A performance comparison between the AXAF telescope and the optimum configuration is given in fig.3.

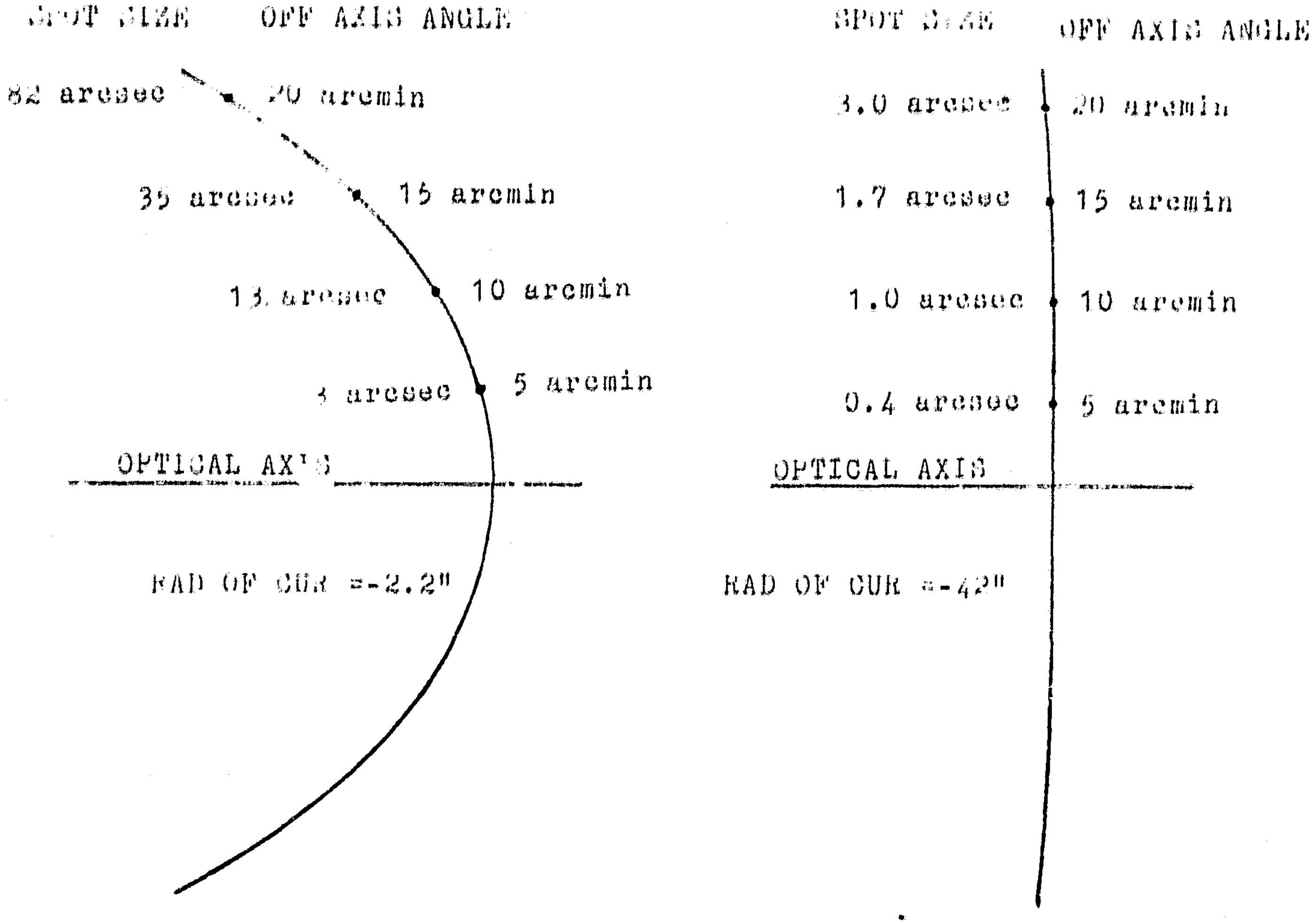

PERFORMANCE OF AXAF

PERFORMANCE OF OPTIMUM CONFIGURATION

Fig.3: Performance comparison

ORIGINAL PAGE IS
OF POOR QUALITY

Figure 4 shows the approximate number of elements (subsystems) and the performance trend of a nested system of grazing incidence telescopes as a function of the system length.

Common system parameters are:

Outer Radius: 24 in.

Inner Radius: 14 in.

Focal Length: 400 in.

ORIGINAL PAGE IS
OF POOR QUALITY

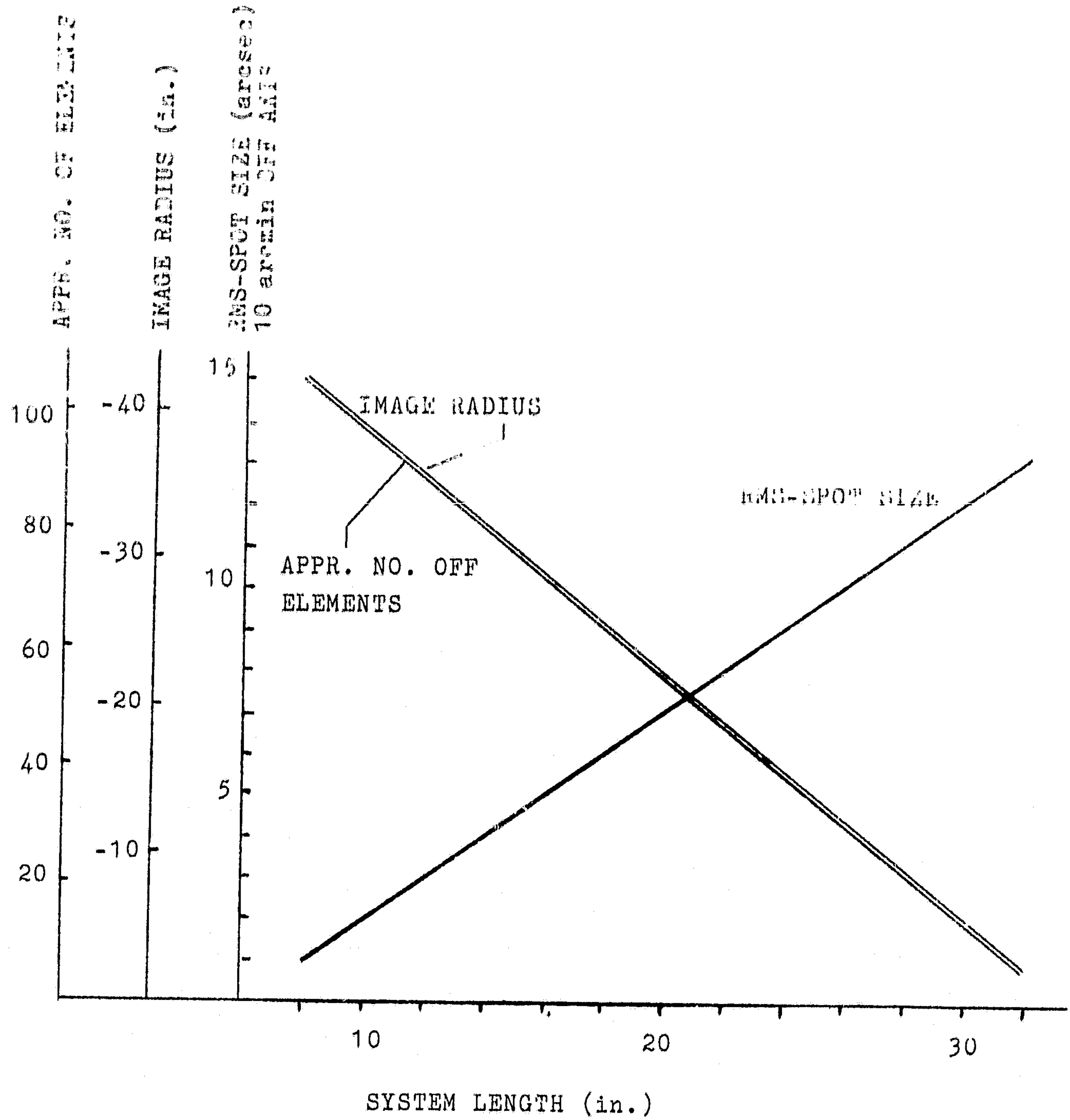

Fig.4: Performance trend as a function of the system length